Available online at www.sciencedirect.com
ScienceDirect
Polymer 47 (2006) 7241–7250
polymer
www.elsevier.com/locate/polymer

Role of main chain rigidity and side-chain substitution on the supramolecular organization of rigid–flexible polymers

P. Riala [a,b], A. Andreopoulou [a,b], J. Kallitsis [a,b,*], A. Gitsas [c,d], G. Floudas [c,d]

[a] Department of Chemistry, University of Patras, University Campus, GR26500 Patras, Greece
[b] Foundation for Research and Technology-Hellas, Institute of Chemical Engineering and High Temperature Processes (FORTH-ICE/HT), Patras 26500, Greece
[c] Department of Physics, University of Ioannina, P.O. Box 1186, 45110 Ioannina, Greece
[d] Foundation for Research and Technology-Hellas, Biomedical Research Institute (BRI)-FORTH, Ioannina, Greece

Received 26 April 2006; received in revised form 4 May 2006; accepted 4 May 2006
Available online 28 July 2006

Dedicated to the memory of the scientist and friend Tadeusz Pakula.

Abstract

The synthesis, characterization and supramolecular organization of rigid–flexible aromatic–aliphatic polyethers are reported. The polymers contain substituted quinquephenyl moieties along their main chains separated by flexible aliphatic units of various lengths. The oligophenylene segments bear different types of dodecyloxy tailed side groups, either attached on the periphery of side dendritic wedges (G_1) or as direct side-chains (G_0). Their structural characterization was performed by means of differential scanning calorimetry, polarizing optical microscopy and X-ray scattering from oriented fibers. These techniques revealed the presence of supramolecular organization in different levels and in the absence of solvent, reflecting a delicate balance of interactions produced by the rigid–flexible backbone segments and the size of dendritic side-chains. It was concluded that the polymers with only two dodecyloxy side-chains (zeroth generation, G_0) possess smectic order. On the other hand, substitution of the quinquephenyl backbone with the dodecyloxy decorated dendrons (first generation, G_1) disrupts the lateral order giving rise to a nematic state. These results are compared with the corresponding rigid–flexible polyethers having terphenyl rigid segments.

Keywords: Rigid–flexible polymers; Supramolecular organization; X-ray

1. Introduction

Over the long history of polymeric materials it has been greatly recognized that the attachment of side groups onto the main backbones is probably the most efficient way in improving their solubility and their processability. Actually, in many of the reported systems, rigid or semiflexible, the wise choice of side substituents has led to macromolecules presenting characteristics not even imagined for their unsubstituted analogues. Some characteristic examples can be found in wholly aromatic polymers in which the attachment of linear side units not only led to improved solubilities [1–5], but also imposed organizational features to the bulk polymeric materials [6–12]. On the other hand, and more recently, side-chain dendronized polymers composed of typical flexible main chains were found to self-organize into various polymorphic structures due to the packing regulations imposed by the number, size and exact chemical structure of the side dendrons [13–20]. A common feature in all these cases can be found in the coexistence of incompatible moieties held tightly together usually through covalent bonding. Thus, the favorable arrangement of same parts together and simultaneously away from different parts is the main factor for the self-organization tendency found in such polymers. This microphase segregation is the

* Corresponding author. Department of Chemistry, University of Patras, University Campus, GR26500 Patras, Greece. Tel.: +30 2610997121; fax: +30 2610997122.
E-mail address: j.kallitsis@chemistry.upatras.gr (J. Kallitsis).

0032-3861/$ - see front matter © 2006 Elsevier Ltd. All rights reserved.
doi:10.1016/j.polymer.2006.05.079

driving mechanism of the increased organization in most liquid crystalline materials, polymeric or oligomeric. Order coming from the rigid parts and mobility from the flexible ones allow the system in adopting the energetically favorable state which leads to self-organization [21–23].

Among the many technological fields that directly benefited from the development of processable, micro-segregated and self-organizable materials are those connected with various optoelectronic applications. The combination of optical properties with supramolecular organization is an important tool in order to modulate the light emission. In view of this, substituted quinquephenyl moieties have been efficiently used as blue light emitters [24–26]. In a recent study of the optical properties of rigid–flexible polyethers having dodecyloxy substituted quinquephenyl units in the main chain higher order situations caused lower quantum efficiencies [26]. Furthermore the latter were directly correlated to the specific polymeric structure since the change of the main chain spacers' length from odd to even number of methylene units strongly increased their organization ability by means of better backbone packing.

In the present work we focus on the synthesis, molecular characterization and self-assembly of aromatic–aliphatic polyethers containing substituted quinquephenyl moieties in the main chain. The influence of the substituents on the supramolecular structure is studied using different types of dodecyloxy tailed side groups. For this purpose we employ, differential scanning calorimetry, polarizing optical microscopy and X-ray scattering. These techniques revealed the presence of supramolecular organization in different levels and in the absence of solvent, reflecting a delicate balance of interactions produced by the rigid–flexible backbone segments and the size of dendritic side-chains. These results are compared with the corresponding terphenyl rigid segments. We find that in going from the terphenyl to the quinquephenyl backbone segments disrupts the lateral order in the first generation (G_1).

2. Experimental section

2.1. Materials

Polyethers **PQ-2OC$_{12}$H$_{25}$-*x*** were synthesized as previously described [24]. 1,4-Di[3,5-bis(dodecyloxy)benzyloxy]-2,5-dibromo benzene (**1**) [20], 4-(tetrahydropyran-2-yloxy)-1,1′-biphenyl-4′-ylboronic acid (**2**) [27] and catalyst $PdCl_2$(dppf) [28] were also synthesized according to literature procedures. All chemicals and reagents were supplied from either Aldrich or Merck and were used without further purification, unless noted otherwise. In particular, aliphatic dibromides of $x = 10$, 12 (dibromododecane and dibromoundecane) were recrystallized from methanol and tetrahydrofuran (THF) was distilled from sodium in the presence of benzophenone prior to use. All reactions were carried out under an argon atmosphere.

2.2. Instrumentation

^{1}H and ^{13}C NMR spectra were obtained on Bruker Avance DPX 400 MHz and 100 MHz spectrometers respectively, with deuterated $CHCl_3$ and DMSO with TMS as an internal standard. Gel permeation chromatography (GPC) measurements were carried out using a Polymer Lab chromatographer with two Ultra Styragel linear columns with pore sizes of 10^4 and 500 Å, UV detector (254 nm), polystyrene standards and $CHCl_3$ as eluent, at 25 °C with a flow rate of 1 mL/min.

DSC experiments were made using a TA Instrument DSC Q100 Series calorimeter with a cell purged with nitrogen (cooling and heating rates of 10 K/min). Calibration for the temperature and enthalpy scales was performed using an indium standard. The melting temperatures (T_m) were obtained from the second heating run that is considered to better reflect the equilibrium properties of the bulk materials.

Wide-angle X-ray scattering (WAXS) measurements were made using a pinhole collimation and a two-dimensional (2D) detector (Siemens A102647) with 1024×1024 pixels. The Cu Kα radiation from a Siemens generator and a graphite monochromator was used ($\lambda = 0.154$ nm). The sample-to-detector distance was 7.05 cm. Measurements were made from macroscopically oriented (extruded) filaments with a diameter of 0.7 mm at different temperatures. In all patterns the filament axis had a vertical orientation with the X-ray beam perpendicular to the filament. The scattered intensity distributions were subsequently integrated along the equatorial and meridional axes and the resulting intensities were plotted as a function of the scattering wave vector q ($=(4\pi/\lambda)\sin(2\theta/2)$, where θ is the scattering angle).

A Zeiss microscope equipped with a Linkam THM600 hot stage was used for the investigation of the optical textures. All samples were cooled from 473 K at 2 K/min to 303 K and the images were recorded with a CCD camera.

Optical absorption spectra were recorded on a Hewlett Packard 8452A spectrophotometer. Photoluminescence spectra were recorded using a Perkin Elmer LS45 luminescence spectrometer, by the excitation of the sample at the absorption maxima of the UV–vis spectra.

2.3. Monomer and polymer synthesis

2″,5″-Di[3,5-bis(dodecyloxy)benzyloxy]-*p*-quinquephenylene-4,4‴-diol, **II(4OC$_{12}$H$_{25}$)**: a degassed mixture of **1** (3.00 g, 2.53 mmol), **2** (4.00 g, 12.75 mmol), $PdCl_2$(dppf) (0.11 g, 0.15 mmol), distilled THF (150 mL) and NaOH (3 N) (10 mL, 30 mmol) was stirred at reflux for 48 h. After cooling to room temperature the organic layer was separated and filtrated for catalyst removal. The organic solvent was evaporated and MeOH was added to precipitate the THP-protected monomer. The white-gray powder was filtrated, washed with MeOH and dried under vacuum giving 2.2 g (56% yield).

The THP-protected monomer was dissolved in THF (60 mL) and then camphorosulfonic acid (CSA) (6.0 g, 25.8 mmol) and MeOH (3 mL) were added under argon atmosphere. The mixture was stirred at room temperature for 48 h, and then precipitated in MeOH (400 mL), filtrated, washed with MeOH and dried under high vacuum. Recrystallization from toluene afforded 1.30 g (76%) of macromonomer diol **II(4OC$_{12}$H$_{25}$)** (Scheme 1). ^{1}H NMR ($CDCl_3$): 0.86 (s, 12H,

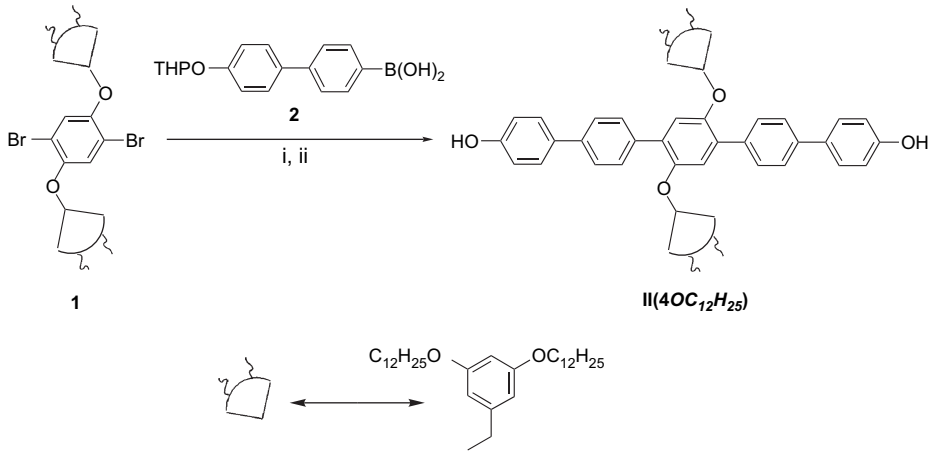

Scheme 1. Syntheses of macromonomer diol **II(4OC$_{12}$H$_{25}$)**. (i) $PdCl_2$(dppf), THF, NaOH 3 N, 70 °C, 48 h, 56%. (ii) CSA, THF, MeOH, 48 h, 76%.

CH_3), 1.24 (s, 72H), 1.65 (s, 8H), 3.81 (s, 8H), 4.98 (s, 4H), 6.33 (s, 2H), 6.45 (s, 4H), 7.11 (s, 2H), 6.92 (d, 4H), 7.52 (d, 4H), 7.60 (s, 4H), 7.67 (s, 4H).

Polyethers **PQ-4OC$_{12}$H$_{25}$-*x***: to a carefully degassed mixture of **II(4OC$_{12}$H$_{25}$)** (0.20 g, 0.15 mmol) the respective aliphatic dibromide (0.15 mmol) and *tert*-butylammonium hydrogen sulfate (TBAH) (20 mg, 0.058 mmol) were added *o*-DCB (1 mL) and NaOH (10 N) (1 mL). The mixture was vigorously stirred under a continuous stream of argon at 120 °C for 2 days. $CHCl_3$ was then added, and the polymer was obtained after precipitation in a 10-fold amount of MeOH, filtration, and drying under vacuum (Scheme 2). **PQ-4OC$_{12}$H$_{25}$-12**: ^{1}H NMR ($CDCl_3$): 0.79 (t, 12H), 1.25–1.33 (two br, 88H), 1.64 (t, 8H), 1.83 (br, 4H), 3.82 (t, 8H), 3.99 (br, 4H), 4.98 (s, 4H), 6.34 (s, 2H), 6.56 (s, 4H), 6.97 (d, 4H), 6.99 (s, 2H), 7.56 (d, 4H), 7.60 (d, 4H), 7.68 (d, 4H).

3. Results and discussion

3.1. Synthesis and thermal properties

Employing the macromonomer approach towards side-chain dendritic polymers we successfully synthesized a quinquephenyl diol **[II(4OC$_{12}$H$_{25}$)]** bearing two alkoxy substituted side dendrons of the first generation (G_1) [29–31]. This diol was used for the preparation of aromatic–aliphatic polyethers under phase transfer polycondensation with aliphatic dibromides of various lengths ($x = 7$–12) [32,33]. In all cases dendronized polymers of high molecular weights were obtained that presented good solubilities in common organic solvents like chloroform. Their structural characterization was performed by means of NMR spectroscopies (Fig. 1) and their molecular characteristics were evaluated using gel permeation chromatography (Table 1). Even though the GPC technique is known to substantially underestimate the true molecular weights of dendronized polymers [19,33] the polymerization degrees calculated for this polymeric series were adequately high. Moreover, no end groups were detected in their ^{1}H NMR spectra (Fig. 1) and also these polymers could easily form self-standing, stable films after solution casting.

Another interesting feature of these dendronized polyethers is the incorporation of quinquephenyl aromatic segments along the main polymeric backbones which are known to impose excellent optoelectronic properties onto the final materials. Particularly, blue light emission has been detected for analogous quinquephenyl polymers bearing aliphatic side-chains or even poly(benzyloxy) side dendrons. In all those previously reported cases such polymers could emit blue light with high quantum yields not only from their dilute solutions but most importantly from their solid states. Additionally, the

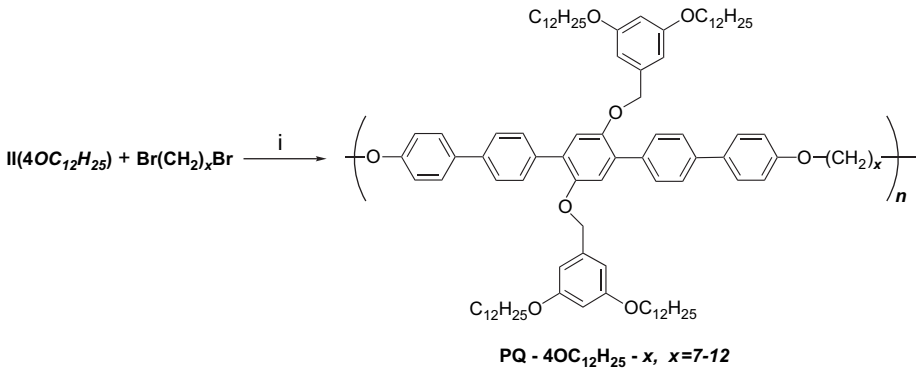

Scheme 2. Syntheses of polyethers **PQ-4OC$_{12}$H$_{25}$-*x***. (i) *o*-DCB, NaOH 10 N, TBAH, 120 °C, 2 days.

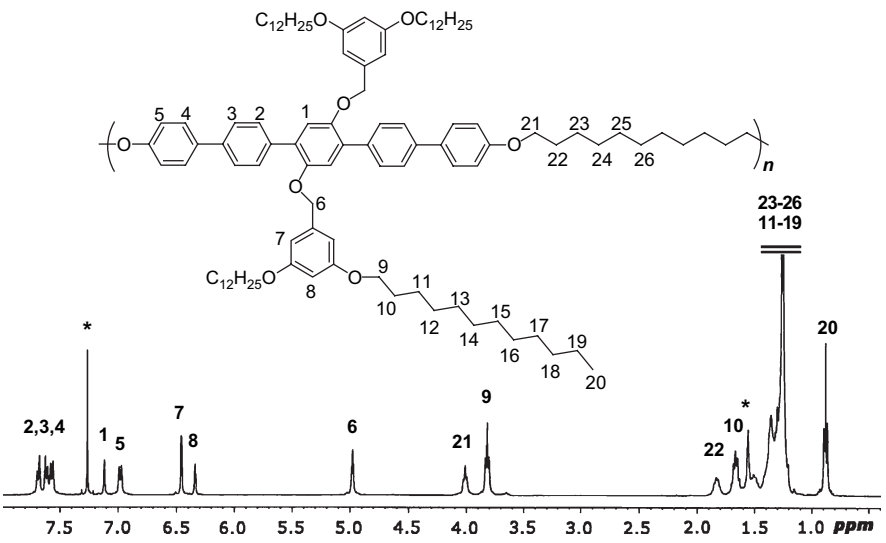

Fig. 1. NMR spectrum of PQ-4$OC_{12}H_{25}$-11 with the assignment of the various peaks.

Table 1
Molecular characteristics of polyethers **PQ-4$OC_{12}H_{25}$-*x*** (first generation, G_1)

x	$\overline{M}_n$ [a]	$\overline{M}_w$ [a]	$\overline{M}_w/\overline{M}_n$ [a]	M_{ru} [b]	DP[c]
7	17 300	63 000	3.6	1456	11.9
8	38 700	117 700	3.0	1472	26.3
9	33 000	116 600	3.5	1486	22.2
10	14 900	38 100	2.6	1500	9.9
10	22 300	52 100	2.3	1500	14.9
11	12 000	38 600	3.2	1514	7.9
11	21 500	40 200	1.9	1514	14.2
12	17 000	65 800	3.9	1528	11.2

[a] Obtained by SEC with UV detector, $CHCl_3$ solvent and PS standards.
[b] M_{ru} is the molecular weight of the monomer unit.
[c] Degree of polymerization calculated by dividing M_n with the respective M_{ru}.

exact length of the intermediate connective aliphatic units has been shown to strongly influence the polymers' luminescence quantum yields [24–26].

A first optical examination of the PQ-4$OC_{12}H_{25}$-*x* polymers has shown that regardless of the flexible spacer length an emission maximum at 406 nm was obtained both in solution and in the solid state. A detailed study of the spacer length on the optical properties and more specifically on the luminescence quantum yield is in progress. However, the influence of the substituents on the luminescent spectra can be obtained by comparison of the PQ-4$OC_{12}H_{25}$-*x* polymers with PQ-2$OC_{12}H_{25}$-*x* (see Scheme 3 and Table 2) and also the same polymeric main chains having two second generation benzyloxy type side dendrons [27]. Depending on the substituent type, a small variation of the emission maxima from 418 nm

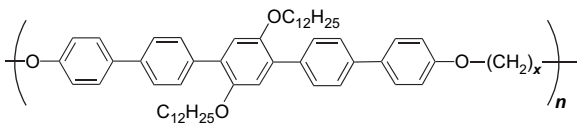

PQ - 2$OC_{12}H_{25}$ - *x*, *x*=7-12

Scheme 3. Structure of polyethers and **PQ-2$OC_{12}H_{25}$-*x***.

Table 2
Molecular characteristics of polyethers **PQ-2$OC_{12}H_{25}$-*x*** (zeroth generation, G_0)

x	$\overline{M}_n$ [a]	$\overline{M}_w$ [a]	$\overline{M}_w/\overline{M}_n$ [a]	M_{ru} [b]	DP[c]
12	67 000	130 500	2	948	70.7
11	49 000	100 000	2	934	52.5

[a] Obtained by SEC with UV detector, $CHCl_3$ solvent and PS standards.
[b] M_{ru} is the molecular weight of the monomer unit.
[c] Degree of polymerization calculated by dividing M_n with the respective M_{ru}.

for PQ-2$OC_{12}H_{25}$-*x* [24] to 406 nm for PQ-4$OC_{12}H_{25}$-*x* and a double peak with maxima at 398 and 420 nm for the second generation benzyloxy analogues [27], were obtained. In all the cases blue light emitting polymers were synthesized but the quantum yields were dependent on the flexible spacer length [26,27].

Thermal analysis was employed as a first insight into their ability to form organized structures. The DSC traces of the PQ-4$OC_{12}H_{25}$-*x* series obtained during the second heating run are depicted in Fig. 2. Depending on the length of the flexible spacer single or multiple transitions are obtained in the range of 393–423 K. The odd members show broad, ill-defined transitions revealing their lower ability for self-organization as compared to the even members where sharper transitions were obtained (this is especially the case for $x = 12$). Nevertheless, there is a general trend towards decreasing melting temperatures with increasing spacer length. For the polyethers with 10 and 11 methylene units, multiple endotherms were obtained that are more pronounced in the former with an even number of methylene units. The thermal behaviour of the monomeric diol [II(4$OC_{12}H_{25}$)] is depicted in Fig. 3 and displays two endothermic peaks during the heating runs. Besides the main melting transition at about 446 K, a weak endothermic peak is observed at ~323 K during the second heating run. Comparing this behaviour with that of the respective diol with the three phenylene rings [34], an increase in the main transition temperature is observed that is expected by the increase in the conjugation

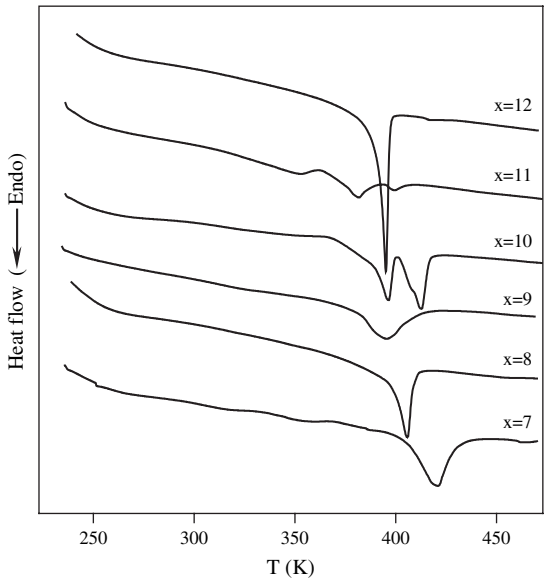

Fig. 2. DSC traces of the PQ-4$OC_{12}H_{25}$-x, $x = 7-12$ series obtained during the second heating run (rate = 10 K/min). Notice the narrower transitions for the even members ($x = 8$, 10, 12) suggesting increased order for $x = 12$.

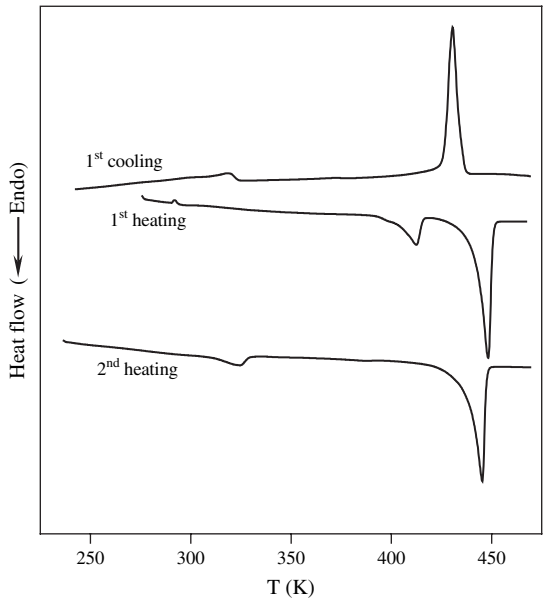

Fig. 3. DSC traces of the macromonomer diol II(4$OC_{12}H_{25}$) obtained during the first heating and cooling runs as well as during the second heating run (rate = 10 K/min).

length. Nevertheless, the first transition at 323 K, is in the same range supporting the notion that is mostly related to the dodecyloxy side-chains.

The influence of the molecular parameters on the highest transition temperatures (T_m) is summarized in Fig. 4. For the same backbone, changing the substituents from dodecyloxy side-chains (G_0) to the first generation dodecyloxy decorated dendrons (G_1), T_m produces a small decrease which is attributed to the dilution effect by the increasing density of the more flexible dodecyloxy side groups in the latter. Alternatively, for the same type of the dendritic substituents (first generation

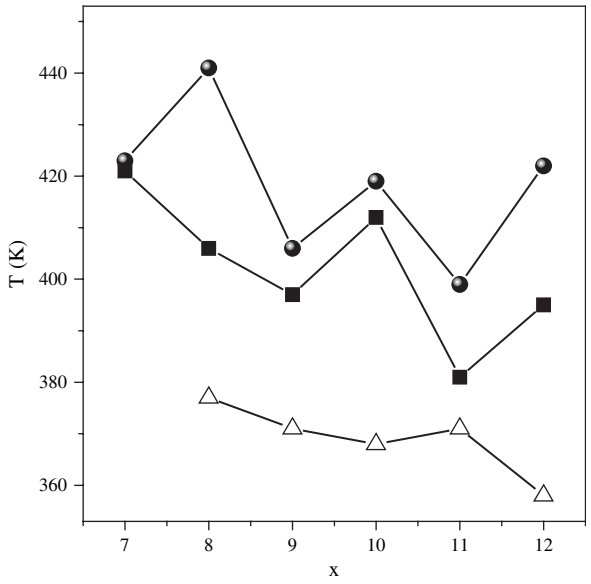

Fig. 4. Variation of the melting temperatures (T_m) obtained from the second heating run plotted vs. the number of methylene units along the backbone (x) for PQ-4$OC_{12}H_{25}$-x (■), PQ-2$OC_{12}H_{25}$-x (●) and PETH-4$OC_{12}H_{25}$-x (△) (the latter from Ref. [9]). Notice the increase of the transition temperatures with increasing backbone rigidity.

quinquephenyl (PQ) and terphenyl (PETH) series) increasing the length of the rigid part in the main chain from terphenyl to quinquephenyl, results in a significant increase of T_m. This is suggestive of a higher order in the PQ series with the more rigid quinquephenyl segments. In all cases an odd–even effect is observed which is more evident in the case of the dodecyloxy substituted polyethers.

3.2. Structure analysis

3.2.1. Macromonomer diol II(4$OC_{12}H_{25}$)

The main feature in the DSC trace from the macromonomer diol is the strong endothermic peak at 446 K suggesting the melting of the mesophase structure. This temperature is higher than in the corresponding terphenyl diol (~398 K) suggesting the presence of a more ordered mesophase. Furthermore, POM images obtained on cooling from the melt revealed space-filling spherulitic superstructures usually found in systems with propensity for crystallization. The X-ray diffraction pattern from an oriented macromonomer diol fiber is shown in Fig. 5 and confirms the presence of an ordered mesophase. The pattern exhibits strong equatorial reflections suggesting a columnar structure and some meridional reflections indicative of periodicities along the filament. The equatorial and meridional integrated intensities (also shown in Fig. 5) further suggest a rectangular lateral ordering with the following periodicities: $d_{100} = 2.9$ nm, $d_{010} = 1.44$ nm and $d_{001} = 0.46$ nm (from the wide-angle meridional reflection). It is worth noticing that the d_{100} spacing is considerably higher than in the corresponding terphenyl diol ($d_{100} = 2.37$ nm) revealing that the increase in backbone length and rigidity poses higher constraints on the possible conformations of the dendritic side-chain substituent

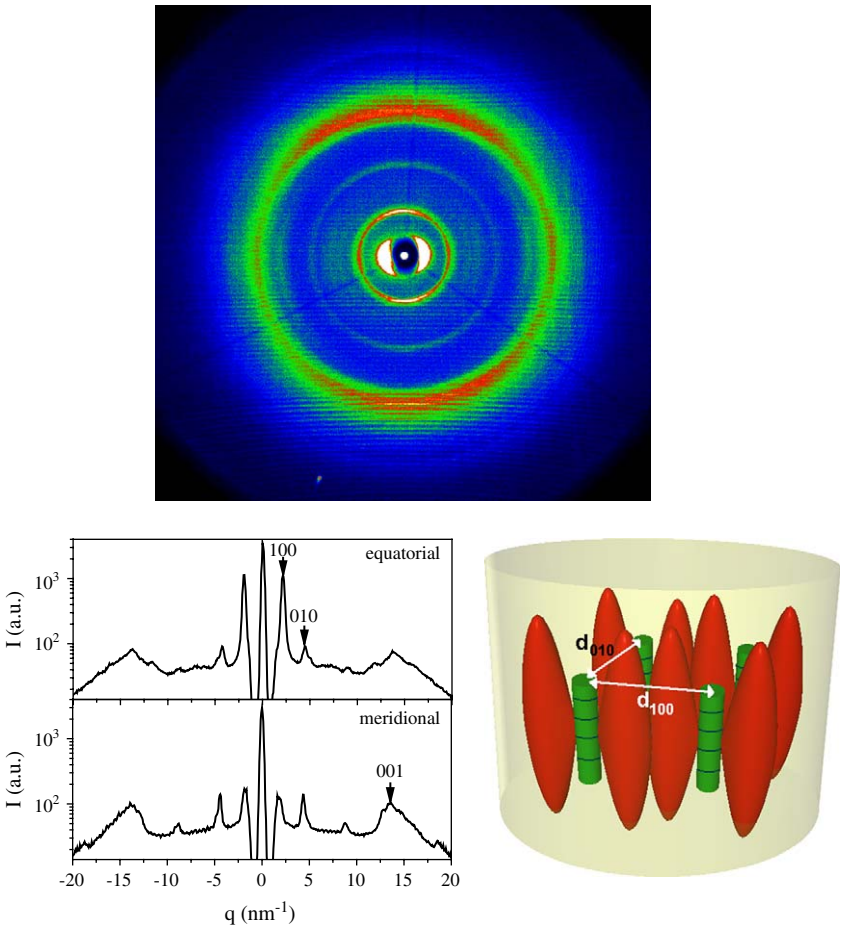

Fig. 5. Top: two-dimensional wide-angle X-ray diffraction pattern from an oriented macromonomer diol fiber. The sample was extruded at 323 K and measured at 303 K. The meridional and equatorial axes are shown with dotted lines. Bottom left: equatorial and meridional intensity profiles obtained from the 2D pattern. The positions from some *hkl* indices corresponding to a rectangular lateral ordering are shown. Bottom right: structure in a macromonomer diol extruded fiber shown in a highly schematic way; the cylinder axis corresponds to the fiber axis. The quinquephenyl (green cylinders) and the $4OC_{12}H_{25}$ side groups (red substituents) are shown. Arrows give the d_{100} and d_{010} periodicities of the rectangular lattice. (For interpretation of the references to colour in this figure legend, the reader is referred to the web version of this article.)

giving rise to an increasing lateral spacing. The approximate organization within the fiber of a macromonomer diol is shown in a highly schematic way in Fig. 5.

3.2.2. Zeroth generation (G_0)

Samples PQ-$2OC_{12}H_{25}$-11 and PQ-$2OC_{12}H_{25}$-12 belong to the zeroth generation (G_0). POM images revealed birefringent structures that most resemble to smectic-like order. However, a definite assignment of the local order requires investigation at the relevant length scale (i.e., X-rays). The diffraction pattern from an oriented fiber of the latter polymer is shown in Fig. 6. The pattern indicates three sets of reflections attributed to periodicities in three perpendicular directions. It exhibits a strong meridional reflection together with some weak higher order reflections revealing a structure composed of alternating quinquephenyl and aliphatic main chain segments. The spacing corresponding to the first intense meridional reflection in PQ-$2OC_{12}H_{25}$-12 is 3.5 nm, i.e., comparable to the backbone length (calculated using Arguslab). The corresponding spacing from the PETH-$2OC_{12}H_{25}$-12 was ~2.8 nm and the increasing periodicity in the former reflects clearly the increase in the backbone length. Position correlations of the quinquephenyl segments in neighboring chains (i.e., within the layers) give rise to the wide-angle equatorial reflection. The set of the first intense equatorial reflections originates from backbone–backbone correlations (i.e., inter-layer periodicity). Based on these reflections from the oriented fibers a layered structure is proposed with smectic order consisting of alternating quinquephenyl and aliphatic chains in the meridional direction and of backbone and of space-filling $OC_{12}H_{25}$ side-chains in the other two directions. The smectic order is driven by the incompatibility of aromatic–aliphatic segments and by the size of side-chains. This type of order in G_0 is shown in a highly schematic way in Fig. 6, together with the expected periodicities.

3.2.3. First generation (G_1)

The WAXS patterns from two fibers PQ-$4OC_{12}H_{25}$-11 and PQ-$4OC_{12}H_{25}$-12 differing only slightly on the spacer length that have been extruded, annealed and measured under identical conditions are compared in Fig. 7. The two images display

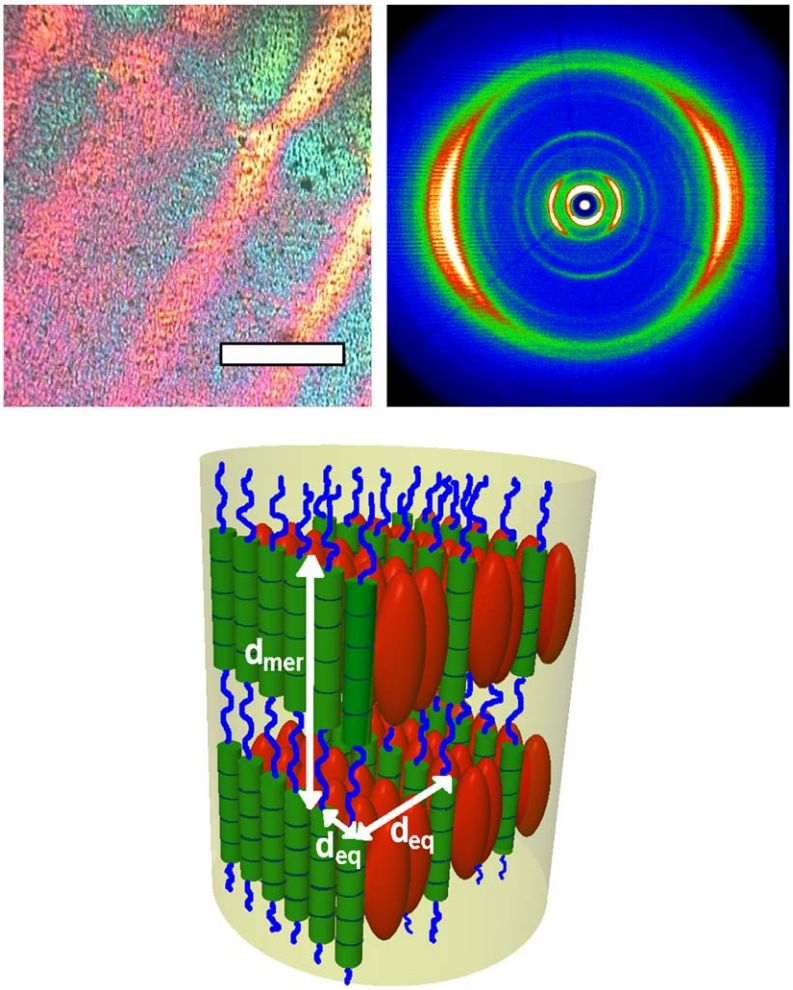

Fig. 6. Top left: POM image from the PQ-2$OC_{12}H_{25}$-12 melt showing birefringence of smectic-like order (the horizontal bar corresponds to 100 μm). Top right: two-dimensional wide-angle X-ray diffraction pattern at 303 K, from an oriented PQ-2$OC_{12}H_{25}$-12 fiber. The sample was extruded at 367 K and subsequently annealed at 353 K for 6 h. The pattern shows strong meridional reflections together with some equatorial reflections. Bottom: schematic of the smectic order within the extruded fiber based on the WAXS pattern. The green cylinder, the blue lines and the red substituent correspond to the quinquephenyl, the aliphatic segments and the 2$OC_{12}H_{25}$ side group, respectively. Arrows indicate the expected equatorial and meridional periodicities. (For interpretation of the references to colour in this figure legend, the reader is referred to the web version of this article.)

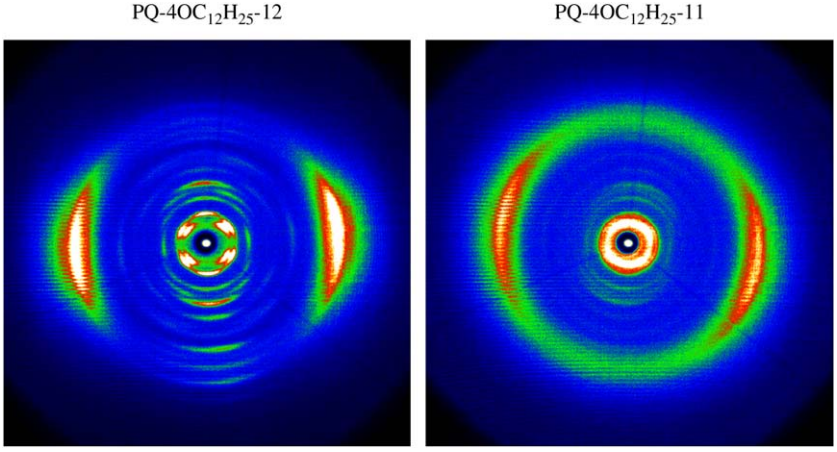

Fig. 7. 2D X-ray diffraction images from oriented fibers of PQ-4$OC_{12}H_{25}$-12 (left) and PQ-4$OC_{12}H_{25}$-11 (right) showing the odd–even spacer length effect on the supramolecular organization. Both fibers were extruded at 323 K and the images were obtained at 303 K following annealing and slow cooling from 383 K. Although both images display some common features the sharp reflections in the former become more diffuse in the latter due to the odd number of spacers.

in general similar scattering features, however, the reflections in the latter, with the even spacer length, are much sharper revealing a very-well ordered structure that is in agreement with the DSC results (Fig. 2). This structural uniformity in all evenly spaced polyethers is attributed to a slightly more compact interchain arrangement that is disrupted in the odd-spaced polymers. This again demonstrates that the molecular organization in these materials rests on a delicate balance of interactions provided by a number of backbone aliphatic segments, the backbone rigidity and the size of side-chains. From these factors it is the number of backbone aliphatic chains (odd–even) that plays the most decisive role in controlling the *degree* of supramolecular order.

The organization within the first generation by increasing the spacer length (PQ-4OC$_{12}$H$_{25}$-*x* series) is shown by the WAXS patterns in Fig. 8. The main characteristic of these images is the presence of intense equatorial reflections and the absence of strong meridional reflections (especially for $x = 7$ and $x = 10$). For $x = 8$ both periodicities are observed, however, the equatorial reflections are the more intense.

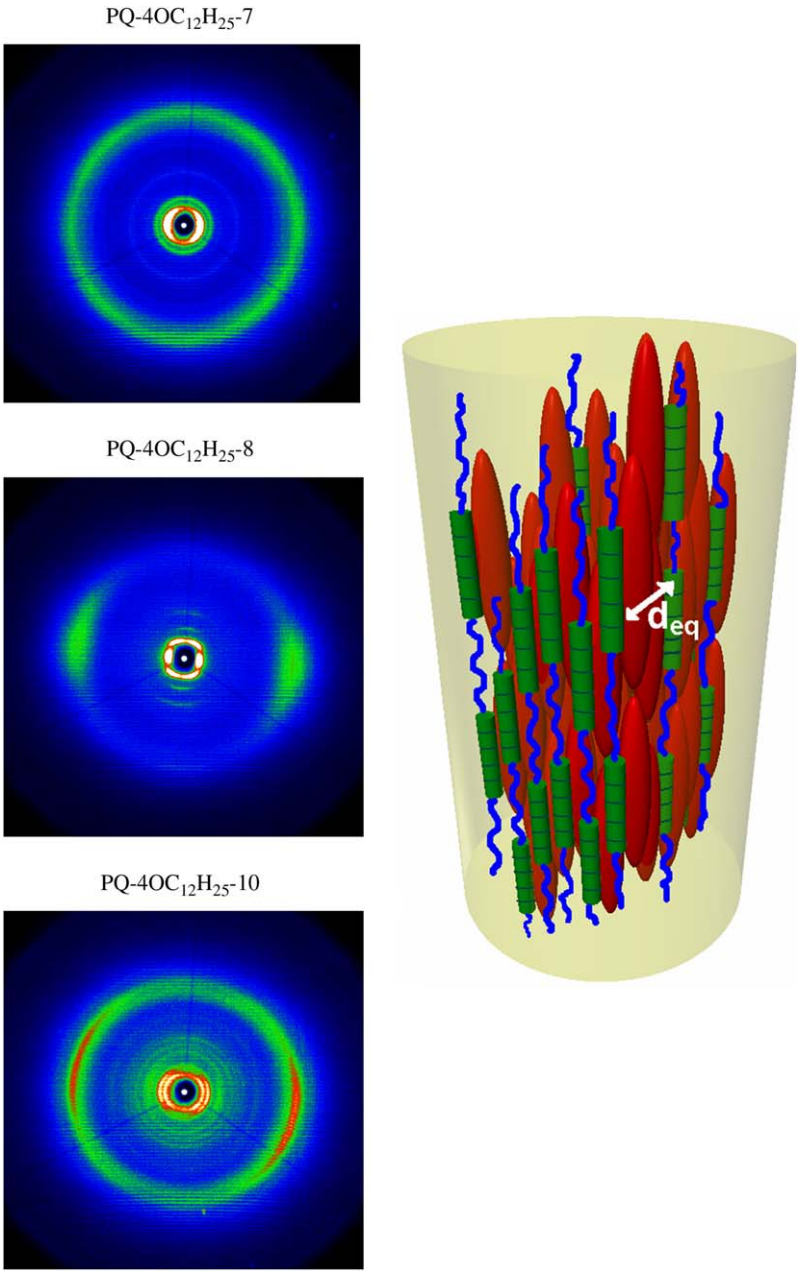

Fig. 8. Left: 2D X-ray diffraction images from oriented fibers of PQ-4OC$_{12}$H$_{25}$-7 (top), PQ-4OC$_{12}$H$_{25}$-8 (middle) and PQ-4OC$_{12}$H$_{25}$-10 (bottom) showing the effect of increasing spacer length. The images are taken at 303 K, following annealing at 373 K. In all cases strong equatorial reflections are observed. Right: schematic representation of the structure in an oriented fiber of the first generation (G_1) exhibiting a nematic order. The green cylinder, the blue lines and the red substituents correspond to the quinquephenyl, the aliphatic segments and the dendritic 4OC$_{12}$H$_{25}$ side group, respectively. The arrow gives the observed equatorial periodicity. (For interpretation of the references to colour in this figure legend, the reader is referred to the web version of this article.)

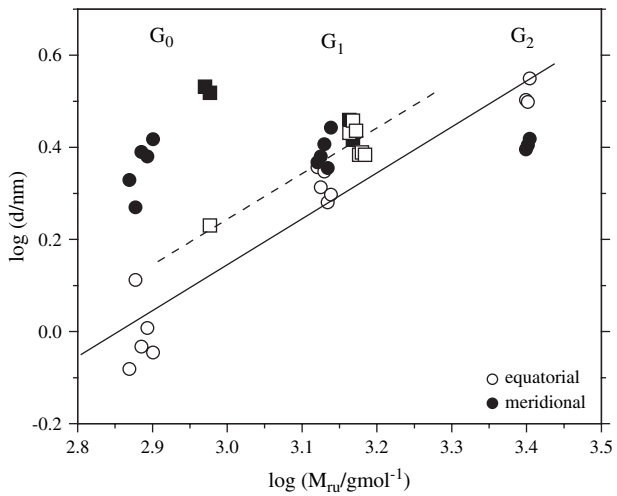

Fig. 9. Dependence of the correlation distances corresponding to the equatorial (open symbols) and meridional (filled symbols) on the molecular mass of the polymer repeat unit (M_{ru}). Data are shown from both the PETH series (circles) and the PQ series (squares). The solid and dashed lines, corresponding to the PETH and PQ equatorial spacings, have a slope of 1 (lines are guides to the eye). The data refer to three generations (G_0, G_1 and G_2) for the PETH series and to two generations (G_0, G_1) for the PQ series.

Furthermore, annealing of the fiber for 12 h at 373 K did not produce any change in the relative intensities suggesting that this is the equilibrium morphology. The presence of strong equatorial reflections and the concomitant absence of meridional reflections suggest a nematic-like order in PQ-4$OC_{12}H_{25}$-*x*. This contrasts with the smectic-like order formed in the PETH-4$OC_{12}H_{25}$-*x* series. This illustrates that the effect of increasing backbone rigidity in going from the terphenyl to the quinquephenyl segments is to disrupt the lateral order and to give rise to a nematic-like order instead. The type of order in G_1 is shown in a highly schematic way in Fig. 8.

3.2.4. Correlation distances – comparison of quinquephenyl (PQ) and terphenyl (PETH) polyethers

The distances determined from the correlations along the backbones (meridional reflections) and correlations between the backbone sheets (equatorial reflections in inter-layers) are compared in Fig. 9 as a function of the molecular weight of the repeat unit. In the same figure we plot the data from the PETH series for the three generations (G_0, G_1 and G_2). The strong meridional correlations along the backbone are longer ranged for the smectic-forming PQ-2$OC_{12}H_{25}$-*x* as compared to PETH-2$OC_{12}H_{25}$-*x* reflecting the larger backbone size in the former. Furthermore, the longer backbone-to-backbone correlations (equatorial spacings) in PQ-2$OC_{12}H_{25}$-12 in comparison to PETH-2$OC_{12}H_{25}$-12 signify the higher restrictions imposed by the increased size and rigidity of the backbone on the side-chain packing. For PQ-4$OC_{12}H_{25}$-*x* (G_1), the structure transforms to nematic, yet the equatorial reflections still provide the backbone-to-backbone correlations that are controlled by the size of side-chains. These correlations are longer ranged as compared to the PETH G_1 series reflecting again the effect of the more rigid backbone.

4. Conclusions

Earlier work has shown that the self-assembly in rigid–flexible polymers composed of aromatic–aliphatic backbone segments can be significantly improved by side-chain substitution. We have studied the self-assembly in newly synthesized aromatic–aliphatic polyethers containing substituted quinquephenyl moieties in the main chain. This appears to be a minor modification of the backbone as compared to the terphenyl rigid segments studied earlier. Furthermore we have studied the influence of substituents on the supramolecular structure using different types of dodecyloxy tailed side groups. Thermal and structural probes revealed the presence of supramolecular organization in the absence of solvent, as with the terphenyl rigid segments. However, going from the terphenyl to the quinquephenyl backbone was found to disrupt the lateral order in the first generation giving rise to a nematic type of order. In addition, a strong effect of the aliphatic spacer length was found (even–odd effect) on the degree of supramolecular order.

These results suggest that the relative ratio of rigid-to-flexible backbone segments and the different sizes of dendritic side-chains create a delicate balance of interactions giving rise to incompatibility and segregation. The *degree* and *type* of order are found to be extremely sensitive to the number of spacer units and the number of phenylene rings along the backbone, respectively.

Acknowledgments

G.F. acknowledges the help by M. Bach with the X-ray measurements and A. Best (MPI-P). This work was partially supported by the Operational Programme for Education and Initial Vocational Training on "Polymer Science and Technology" 3.2a, 33H6, administered through the Ministry of Education in Greece.

References

[1] Majnusz J, Catala JM, Lenz RW. Eur Polym J 1983;19:1043–6.
[2] Majnusz J, Lenz RW. Eur Polym J 1989;25:847–55.
[3] Ballauff M. Makromol Chem Rapid Commun 1986;7:407–14.
[4] Rehahn M, Schlüter DA, Wegner G, Feast J. Polymer 1989;30:1054–9.
[5] Rehahn M, Schlüter DA, Wegner G, Feast J. Polymer 1989;30:1060–2.
[6] Rodriguez-Parada JM, Duran R, Wegner G. Macromolecules 1989;22:2507–16.
[7] Ballauff M, Schmidt GF. Makromol Chem Rapid Commun 1987;8:93–7.
[8] Ballauff M. Angew Chem Int Ed Engl 1989;28:253–5.
[9] Schrauewen C, Pakula T, Wegner G. Makromol Chem 1992;193:11–30.
[10] Kakali F, Kallitsis J, Pakula T, Wegner G. Macromolecules 1998;31:6190–8.
[11] Gitsas A, Floudas G, Wegner G. Phys Rev E 2004;69:041802.
[12] Mierzwa M, Floudas G, Neidhoefer M, Graf R, Spiess HW, Meyer WH, et al. J Chem Phys 2002;117:6289.
[13] Hudson SD, Jung HT, Percec V, Cho WD, Johansson G, Ungar G, et al. Science 1997;278:449–52.
[14] Percec V, Ahn CH, Ungar G, Yeardley DJP, Möller M, Sheiko SS. Nature 1998;391:161–4.
[15] Percec V, Ahn CH, Cho WD, Jamieson AM, Kim J, Leman T, et al. J Am Chem Soc 1998;120:8619–31.
[16] Percec V, Cho WD, Ungar G, Yeardley DJP. J Am Chem Soc 2001;123:1302–15.

[17] Percec V, Cho WD, Mosier PE, Ungar G, Yeardley DJP. J Am Chem Soc 1998;120:11061–70.
[18] Schlüter DA, Zhang A, Okrasa L, Pakula T. J Am Chem Soc 2004;126:6658–66.
[19] Schlüter DA, Rabe JP. Angew Chem Int Ed Engl 2000;39:864–83.
[20] Andreopoulou AK, Carbonnier B, Kallitsis JK, Pakula T. Macromolecules 2004;37:3576–87.
[21] Tschierske C. J Mater Chem 2001;11:2647–71.
[22] Tschierske C. J Mater Chem 1998;8:1485–508.
[23] Demus D, Goodby J, Gray GW, Spiess HW, Vill V, editors. Handbook of liquid crystals. Wiley-VCH; 1998.
[24] Konstandakopoulou FD, Gravalos KG, Kallitsis JK. Macromolecules 1998;31:5264–71.
[25] Kallitsis JK, Gravalos K, Hilberer A, Hadziioannou G. Macromolecules 1997;30:2989–96.
[26] Pistolis G, Malliaris A, Andreopoulou AK, Kallitsis JK. J Phys Chem B 2005;109:11538–43.
[27] Pistolis G, Andreopoulou AK, Malliaris A, Kallitsis JK. Macromolecules 2004;37:1524–30.
[28] Hayashi T, Konishi M, Kumada M, Higushi T, Hirotsu K. J Am Chem Soc 1984;106:158–63.
[29] Zhang A, Shu L, Bo Z, Schlüter DA. Macromol Chem Phys 2003;204:328–39.
[30] Schlüter DA. Top Curr Chem 2005;245:151–91.
[31] Frauenrath H. Prog Polym Sci 2005;30:325–84.
[32] Percec V, Kawasumi M. Macromolecules 1993;26(15):3917–28.
[33] Andreopoulou AK, Kallitsis JK. Macromolecules 2002;35:5808–15.
[34] Carbonier B, Andreopoulou AK, Pakula T, Kallitsis JK. Macromol Chem Phys 2005;206:66–76.